Passive Water–Lipid Peptide Translocators with Conformational Switches: From Single-Molecule Probe to Cellular Assay

ARTICLE *in* THE JOURNAL OF PHYSICAL CHEMISTRY B · JANUARY 2008

Impact Factor: 3.3 · DOI: 10.1021/jp074479u · Source: PubMed

3 AUTHORS, INCLUDING:

Ariel Fernandez
Rice University
310 PUBLICATIONS **3,020** CITATIONS
SEE PROFILE

Axel Blau
Istituto Italiano di Tecnologia
52 PUBLICATIONS **819** CITATIONS
SEE PROFILE

Published in final edited form as:
J Phys Chem B. 2007 December 20; 111(50): 13987–13992. doi:10.1021/jp074479u.

Passive water-lipid peptide translocators with conformational switches: From single-molecule probe to cellular assay

Ariel Fernández[1*], **Alejandro Crespo**[1], and **Axel Blau**[2]

[1]*Department of Bioengineering, Rice University, Houston, TX 77005, USA*

[2]*Fachbereich Physik, Technische Universität Kaiserslautern Erwin-Schrödinger-Straße, Gebäude 46 D-67663 Kaiserslautern, Germany*

Abstract

Peptide design for unassisted passive water/lipid translocation remains a challenge, notwithstanding its importance for drug delivery. We introduce a design paradigm based on conformational switches operating as passive translocation vehicles. The interfacial behavior of the molecular prototype, probed in single-molecule AFM experiments, reveals a near-barrierless translocation. The associated free-energy agrees with mesoscopic measurements, and the *in vitro* behavior is quantitatively reproduced in cellular assays. The prototypes herald the advent of novel nano-biomaterials for passive translocation.

Keywords

peptide; cellular translocation; conformational change; cell membrane; interface

Introduction

The design of peptides soluble in water and in lipid phases poses a major bottleneck to the development of translocation technologies for peptide-based drug delivery[1–3]. In this work we introduce a peptide-design strategy that utilizes a conformational switch as a vehicle for translocation, circumventing the need for active-transport devices. We report on single-molecule probes adapted to investigate the interfacial behavior of peptides endowed with dual solubility. The engineered prototype peptide possesses delocalized charges[4] and is capable of minimizing hydration demands by a “camouflaging” change in conformation concurrent with passive translocation into the lipid phase. Transference from water to lipid promotes a compensatory enhancement of intramolecular electrostatic interactions.

Given the dual-solubility constraint, the peptide must visit two conformations, one soluble in water and the other promoting dehydration. Hence, the peptide involves polar side-chains, hydrated when exposed to water, but capable of engaging in intramolecular electrostatic interactions that promote lipid internalization. This design requires that we identify polar pairs with enough charge delocalization to be favorably transferred to the lipid phase. The highest charge delocalization - and consequently the lowest extent of hydration - in a side-chain cation is found in the guanidinium ion (Gd^+, $(NH_2)_3C^+$)[4]. Thus, we selected the peptide YQDRDARDRNM (peptide 1), capable of forming three guanidinium-carboxyl interactions in a helical conformation that pairs arginine (R) and aspartate (D) side chains with (i, i+4) periodicity. The capping terminal residue pairs YQ and NM were selected to ensure some

*Corresponding author; E-mail: arifer@rice.edu.

degree of helicity in water, based on a similar motif YQDRYYRENM, with two (i, i+4)-guanidinium-carboxyl pairs (D-R and R-E), occurring in helix 1 of the cellular prion protein[5]. The adjacency of opposite-charge amino acids in opposite dipole orientations reduces charge-backbone macrodipole interactions that would overstabilize the helix[6].

To benchmark the significance of charge delocalization in the translocation design, amino acid substitutions R→K, effectively replacing charge-delocalized Gd^+ for charge-localized $-NH_3^+$ (ammonium), will be adopted as control experiments.

We introduce and validate the peptide design strategy by probing the translocating efficiency of a conformational switch with minimal dehydration penalties. This is accomplished by first examining the adsorption/desorption behavior of the molecular prototypes at lipid/water interfaces vis-à-vis the conformational changes inferred from circular dichroism. These mesoscopic measurements are subsequently contrasted against a single-molecule dissection of the interfacial behavior of the peptides achieved through atomic force microscopy. The single-molecule methodology is adapted to probe soft interfaces by affixing the purported translocating molecule to the cantilever tip of the molecular force probe. Our single-molecule results reveal that the peptide with specific sequence Ac-YQDRDARDRNM-NH_2 has a near-barrierless translocating efficiency. The estimation of the insertion free energy parameters by harvesting and averaging irreversible-work single-molecule trajectories is shown to be in quantitative agreement with kinetic and thermodynamic parameters derived from the mesoscopic measurements. Finally, a cell-based assessment of the translocating propensity of the designed peptides is carried out, corroborating the trends determined *in vitro*.

Methods

Circular dichroism

CD spectra were recorded on an Aviv 62DS spectrometer (Lakewood, NJ) at far-UV wavelength range 180–280nm (bandwidth=1nm; step interval=0.5nm; response time=2s). Measurements were performed on synthetic peptides (Sigma, >95% purity) at peptide concentration=0.2mM in Dulbecco's phosphate buffer saline solution (PBS, pH7.2, DuPont de Nemours), in DSPC (1,2-stearoyl-sn-glycero-3 phosphatidylcholine, aliphatic chains length N=18, Avanti) liposomes. The latter were prepared by sonication with the method of Lee et al.[7]. The mean ellipticity [Θ] is reported in deg cm^2/dmol, in accord with previously reported measurements of peptide helicity[8,9]. The percentage helicity (mean residue value) was determined from the CD spectra using the method by Yang *et al.*[10] which deconvolutes from the signal the contributions from helix, sheet, turn and coil, as previously reported for translocating peptides[11].

Adsorption/desorption measurements

Peptide adsorption/desorption onto and from a Langmuir-Blodget DSPC bilayer is measured under controlled hydrodynamic conditions identical to those given in[12], with a constant flux of $5\times10^{-3}cm^3/s$. Adsorption took place at constant bulk concentration 1.5 μM, desorption at 0 μM bulk concentration, and variations in the adsorption uptake for different peptides were monitored using evanescent field total reflection spectroscopy using an optical biosensing device that interrogates a coating of an optical waveguide serving as the floor of the cell. The waveguiding TiO_2/SiO_2 coat is 180nm thick, with a wide diffraction grating of period 412nm (Harrick Scientific), and the evanescent field total reflection makes use of a polarized light beam with wavelength 632.8nm (Spectra-Physics). All measurements were made at T=301K and buffer composition: 10mM Hepes/0.7mM EDTA, pH7.1 (refractive index=1.33303). Changes in refractive index within a layer of thickness 2nm from the waveguide frustrate total reflection and thus become detectable, enabling a direct determination of the number of

internalized peptide molecules per μm^2. The total-reflection spectroscopy set up was also used to probe the bilayer for packing defects in its construction, since such defects perturb the refractive index. Defective bilayers were discarded. At the experimental temperature, the DSPC bilayer is technically in the crystalline phase (reported phase transition temperature ~328K, Avanti), thus introducing the most stringent physical conditions for peptide insertion.

Molecular force probe (MFP)

The MFP-3D™-BIO Atomic Force Microscope (Asylum Research Corp., Santa Barbara) is sensored in all three axes for the lowest noise levels and extremely accurate scanning. The Nanopositioning System (NPS) allows the MFP-3D controller to measure the behavior of the piezo with noise levels that are the lowest of any commercially available instrument (< 0.2 nm absolute deviation (Adev) in a 1 kHz bandwidth in the Z direction, and < 0.4nm in the X and Y directions; sensor non-linearity < 0.1% Adev/Full travel at full scan in a 0.1–1 kHz bandwidth). Motions from microns to ~0.1 Å are measured by the deflection sensor. The "biolever" cantilever BL-RC150VB-HW (Olympus) adopted for the force measurements on the soft samples has a spring constant 6 pN/m (the lowest commercially available), with tip gold coating for functionalization.

Single-molecule attachment protocol

A semirigid single molecule of the thiol-acylated peptide (HS-CH_2-CH=CH-CH_2CO-[YQDRDARDRNM]-NH_2) (Dojindo Molecular Technologies Inc.) was immobilized on the gold-coated silicon nitride tip of the cantilever through an Au-S bond. Single-molecule attachment to the cantilever tip required a combination of the following mechanical and redox chemical steps (Fig. 1). The procedure comprises five steps following deposition of a drop of thio-acylated peptide solution (1mM) onto a freshly evaporated gold surface for gold-thiolate tethering forming a molecular brush: 1) Contacting the droplet with the cantilever tip for molecular adsorption of chains tethered to the sample surface through S-Au bonds. 2) Cantilever retraction inducing sequential and partially overlapping stretching of adsorbed molecules followed by successive detachment signaled by dips in cantilever deflection. The single-molecule adsorption signal is calibrated by the extension trace[13–15]. Cantilever pulling from the brush of acylated peptides tethered to the sample surface and adsorbed onto the tip produces extension traces as successive chains become detached from the cantilever tip[15]. The adsorption technique allows for stable attachment as a pulling force of hundreds of piconewtons is applied over intervals of tens of seconds without the interference of polymer creeping. All molecules are detached as the retraction distance z (from tip to sample) approaches the contour length (18Å)[16] of the thio-acylated peptide. Thus, the retraction deflection curves are calibrated to identify the last trace at z<18Å, before complete detachment from the sample surface[17]. The adsorbed polymer is stretched by retracting the cantilever tip, and in cases where multiple polymers are attached, the tip is gradually removed from the surface until all but the longest polymer adsorbed is ruptured[15]. The "last rupture trace" is confirmed to correspond to a single molecule on account of its shape, reflecting a final sharp dip in deflection force and the reproducibility of this retraction shape[15]. We corroborate that a single molecule is left adsorbed on the tip by noting that its rupture ends all probe-surface interactions. Once the critical distance z=16Å for "sharp last rupture" has been determined, it is adopted to prepare new cantilever tips with single-molecule attachment. 3) Hydroquinone (1mM solution, buffer pH4.8) reduction (lysis) of the thiolate-gold bonds of the chains to the sample surface according to the redox reaction: 2(-S-Au)+$C_6H_6O_2$→2(-SH)+Au+$C_6H_4O_2$. 4) Complete removal of cantilever with adsorbed single molecule from sample and dipping cantilever into oxidative 10mM solution of quinone[14] to promote the reverse redox reaction. 5) Thiolate-gold tethering onto cantilever tip. The single-molecule functionalized tip is subsequently rinsed with ultra-distilled water (Millipore).

The AFM set-up was used to examine the mechanical behavior of translocating peptides as the cantilever approaches the interface between an aqueous buffer (0.01M Hepes, 0.7mM EDTA) and a Langmuir-Blodget DSPC bilayer in a damped-fluctuation regime. The functionalized cantilever is calibrated after the experiments through dispersion-based analysis of the thermal noise spectra, yielding the spring constant value 6.7pN/nm.

Cell translocation assays

Mouse macrophage RAW264.7 cells were cultured [18] at a density of 10^5 cells/dish on 35mm dishes. The incubation medium[18] was changed after 48h for media containing rhodamine-labelled conjugate derivatives (Invitrogen, absorption wavelength 548nm, emission wavelength 611nm) of the designed peptides at 1μM concentration. Incubation with the fluorophore-containing media for 1h and 4h was followed by twice washing with PBS (phosphate buffer saline) and final exposure to a PBS solution with 5% lysing agent Triton X-100. The lysate was centrifuged and the fluorescence intensity of supernatant was determined. Peptide uptake was determined on cells incubated as described above for 1h and 4h. The uptake was also determined on cells treated with trypsin (1mg/ml) for a 15 min-digestion of labeled peptides bound to the cell membrane at the end of each incubation period, and also on cells incubated with 5mM sodium azide/10mM 2-deoxy D-glucose for 1 hr prior to incubation with the labeled peptide solution. Trypsin digestion removes membrane-bound peptides, while the sodium azide treatment depletes cellular ATP.

Results and Discussion

1. Solvent-dependent conformational switch

The percentage helicity (mean residue value) of peptides Ac-YQDRDARDRNM-NH_2 (peptide 1) and Ac-YQDRDARDKNM-NH_2 (peptide 2) in water (acylation and amidation removes terminal backbone charges), as determined by signal deconvolution[10] of circular dichroism spectra (Fig. 2)[7–10], is 11%, 18%, respectively. The low helical content reflects the propensity of isolated polar groups to maximize hydration. Helicity increases (82%, 76%, respectively) in DSPC (di-stearoyl- phosphatidylcholine) liposomes, in accord with the compensatory effect introduced by the enhancement of side-chain electrostatic (i, i+4)-interactions in the anhydrous phase. The signal for peptide 1 in lipid phase is the one that best approximates the helical profile (ref. 9, Fig. 1).

2. Mesoscopic assessment of insertion propensity

We assay for dual solubility by determining the adsorption kinetics of each peptide onto a neutrally charged Langmuir-Blodgett DSPC lipid bilayer under controlled hydrodynamic conditions for the peptide solution (Fig. 3)[12]. The DSPC film is mounted onto a waveguide for total reflection[12] with an evanescent field penetration depth of 2nm. The evanescent-field sensor detects changes in refractive index of the lipid phase due to peptide insertion and thus enables a quantification of the peptide uptake through the assessment of perturbations to total reflection. Fig. 3 reveals significant adsorption and detectable internalization of peptide 1, since the 2nm-penetration depth of the evanescent field is approximately half the thickness of the bilayer (~44Å). Upon R→K substitution, the equilibrium uptake is reduced by an order of magnitude, and a double R→K substitution (producing peptide 3: Ac-YQDRDAKDKNM-NH_2) makes adsorption or internalization almost undetectable (Fig. 3). Peptides 1, 2 are clearly able to translocate, as reflected in their full desorption on timescales comparable to those of adsorption equilibration. The equilibrium uptake ratio L_2/L_1=9.79±2.36 for peptides 1 and 2 yields the thermodynamic parameter reflecting the effect of charge delocalization on peptide internalization: $L_2/L_1 = \exp(-\Delta\Delta G/kT)$ (k=Boltzmann constant, T=absolute temperature=301K), with $\Delta\Delta G=\Delta G_2-\Delta G_1$=2.28±0.78kT. ΔG_1, ΔG_2 are the free energy changes associated with transference to an anhydrous phase for peptides 1 and 2, respectively.

This estimation of ΔΔG will be validated by contrasting it with a single-molecule determination.

The difference E_{a2}-E_{a1} of activation-energy barriers for internalization is obtained from initial adsorption velocities, v_1 and v_2. Initial velocities follow unimolecular kinetics subsequently distorted by parking and lateral effects on the bilayer. Thus, $v_1/v_2=(f_1/f_2)\exp[(E_{a2}-E_{a1})/kT]$, where, in accord with general theory of rate process, f_1 and f_2 are pre-exponential factors representing the frequencies of enabling collision at the water-lipid interface for peptides 1 and 2, respectively. An enabling collision promotes the furtherance of the rate process hence, in the particular case under study, it leads to peptide internalization. Peptide chains may collide with the lipid interface but insertion requires the helical conformation, and thus an enabling collision is one in which the chain is helical at the instant when the encounter takes place. Thus, we can introduce the estimate $(f_1/f_2)\approx(\phi_1/\phi_2)$, where ϕ_1, ϕ_2 are the respective percentage peptide helicities in water (Fig. 2). This estimate is justified since the helical conformation has a propensity for dehydration. The validity of the resulting estimation of E_{a2}-E_{a1} = *ln* [4.7×0.38/(0.07×0.41)]±0.80kT = 3.81±0.80kT will be established by comparison with single-molecule determinations.

3. Single-molecule experiments

The mechanistic interfacial behavior of the designed peptides was investigated at the single-molecule level through atomic force microscopy (AFM) using a gold-coated cantilever with spring constant 6pN/nm, adequate to probe soft samples. The peptides were acylated at the N-terminus with a thiolated semirigid spacer yielding the molecule: HS-CH_2-CH=CH-CH_2CO-[YQDRDARDRNM]-NH_2 (contour length[16]: 18.0Å). The tethering of a single molecule to the cantilever tip required five steps (Methods), coupling insertion/retraction cycles into and from a brush of molecules tethered to a gold sample surface with redox hydroquinone/quinone chemistry[14]. The redox steps are required for single thiolate-gold bond swapping from sample surface to cantilever tip. We first verified that a single molecule was left adsorbed on the cantilever tip by noting that its rupture removed any probe-surface interaction. Thus, a critical distance z=16Å for “sharp last rupture” was first determined and then further adopted to assemble cantilever tips with single-molecule attachment.

The deflection force acting on the cantilever upon penetration or retraction into and from a DSPC bilayer is recorded as the water-lipid interface is probed with the thiol-acylated peptide tethered to the cantilever tip (Fig. 4). The deflection force f is recorded as function of cantilever displacement, z, given by the distance between the cantilever tip and the interface. The work $W_{(z)}=-\int_{[z,18Å]}f(z')dz'$ was obtained for each insertion and retraction curve in each cycle performed at constant steering speed. The peptide mechanical behavior was probed at speeds 0.1, 0.06, 0.05 and 0.04 nm/s, collecting 40 cycles for each speed. The data collection was distributed equally on four cantilever tips prepared as indicated in Methods. Each tip was used to generate 40 insertion/retraction cycles, 10 for each speed. The results are reproducible in so far as the free energy estimations based on irreversible trajectories are indistinguishable within the confidence band dictated by thermal fluctuations. The three lowest speeds yielded 85–90% irreversible trajectories with significant hysteresis (above thermal fluctuations), marked by $|W_{pen}-W_{ret}|>kT$, with W_{pen} and W_{ret} being penetration and retraction work. The penetration curve in such trajectories presents a repulsive bump at around z=12.5Å, likely corresponding to an unsuccessful collision between the unfolded and highly polar peptide and the lipid/water interface. This bump is followed by an attractive well at z=11.0Å, signaling lipid solubilization of the hydrophobic conformation promoted by helical conversion (cf. Fig. 2, Fig. 4). The f-z curve becomes monotonically repulsive for z<9Å, as the polar acyl-N-terminus junction approaches the lipid interface. The retraction trajectories reveal an attractive well in the range 9–15Å, a result of the lipid solubility of the helical conformation, dominant in the lipid phase

(Fig. 2). About 15–10% of the trajectories produce minimal work obeying $|W_{pen}-W_{ret}|<kT/2$, and thus approach reversibility. Similar statistics hold for the R→K substituted peptide 2 (Fig. 5), with less than 5% of trajectories free from hysteresis.

An estimation ΔG_J of the free energy profile $\Delta G(z)$ was obtained using Jarzynski's equality $\exp(-\Delta G(z)/kT)=\langle\exp(-W(z)/kT)\rangle$, where $\langle\ \rangle$ denotes an average extended over all trajectories over which irreversible work W(z) is performed[19–21]. Because of the exponential sampling, the trajectories with dominant weight correspond to those with minimal work, that is, the trajectories that most closely approach the reversible trajectory (the quasi- reversible cycles are indicated in blue lines in Fig. 4, 5). For the three lowest steering speeds (0.06, 0.05 and 0.04 nm/s), the penetration and retraction ΔG_J-values were found to be within kT/2 in the range 9Å <z<17Å and for peptides 1 and 2. Furthermore, the ΔG_J-values extracted from each of the three speed manifolds agreed to within kT/2 for the two peptides. These agreements validate the estimation procedure.

The ΔG_J-values shown in Fig. 6 correspond to the low-speed 0.04nm/s manifold for each peptide. The high-speed manifold (0.1nm/s) was discarded in all cases since it revealed a significant discrepancy ($Max_{9<z<17}|W_{pen}-W_{ret}|>k_BT$) and produced no hysteresis-free trajectory. The actual penetration of peptides 1 and 2 into the lipid bilayer is corroborated by comparison with the free energy profile of peptide 3. The higher positive charge localization is clearly precluding penetration for this peptide (cf. Fig. 3), as evidenced by a monotonic increase in ΔG_J which already starts at z-values comparable to the contour length (18Å). This monotonic increase of the free energy stands in contrast with the free energy profiles of peptides 1 and 2 that encounter an attractive well for z-values comparable to the contour length of the spacer (9Å), thus signaling peptide insertion into the lipid phase (Fig. 6). Furthermore, within experimental uncertainty, peptide 3 reveals no hysteresis in any trajectory ($W_{pen}\approx W_{ret}$), another indication that it remains in the aqueous phase.

The single-molecule free energy profiles yield an estimated $\Delta\Delta G=2.55\pm0.5$ kT resulting from the difference in ΔG_J at the well minima for peptides 1 and 2. This single-molecule determination fully agrees within experimental uncertainty with the macroscopic value $\Delta\Delta G=\Delta G_2-\Delta G_1=2.28\pm0.78$kT. Furthermore, the insertion of peptide 1 into the lipid is shown to occur with no detectable barrier ($E_{a1}\approx0$) and is essentially reversible ($\Delta G\approx-1.0$kT), in accord with the purported translocating propensity. The kinetic parameter $E_{a2}-E_{a1}\approx E_{a2}$ is estimated at 4.02±0.88kT from the single-molecule measurements (Fig. 4), in good agreement with the macroscopic value $E_{a2}-E_{a1}=3.81\pm0.80$kT.

4. Peptide translocation in cells

The established *in vitro* trends for translocation were further tested by assaying for peptide translocation in cells. Thus, the superior translocation efficiency of peptide 1 (sequence YQDRDARDRNM) was established through cell-internalization assays using fluorescent-labeled peptides (Fig. 7). Our controls show no internalization of the isolated fluorophore or labeled random peptides of the same length as the designed prototypes. A comparison with peptides 2 and 3 (respective sequences YQDRDARDKNM, YQDRDAKDKNM), with the same charge distribution but lower extents of charge delocalization, reveals that the highest extent of cellular incorporation occurs for peptide 1. None of the three peptides is likely internalized through an endocytosis active mechanism, as revealed by the insensitivity of the cellular uptake to ATP-depletion in the cell (Fig. 7), but rather through passive diffusion, in accord with our *in vitro* and single-molecule results. Furthermore, as demonstrated by trypsin digestion, only a mere 12±6% of the cellular uptake for peptide 1 might be attributed to membrane insertion without internalization (Fig. 7).

Concluding remarks

The agreement between macroscopic and single-molecule measurements of the passive translocation of conformation-switching peptides attests to the correctness of Jarzynski's equality to obtain translocation free energies. Moreover, the work reports on the first use of AFM technology to probe translocation events across soft interfaces.

Our results support a paradigm for the design of peptide translocators. The strategy is based on building a conformational switch that mechanistically promotes the crossing from water into a lipid phase without resorting to active transport machinery and with minimal dehydration penalties. These conformation-switching peptides will likely inspire novel biomaterials capable of passive translocation.

Acknowledgements

The research of A. F. is supported by NIH grant 1R01 GM072614 (NIGMS), by the John and Ann Doerr Fund for Computational Biomedicine, and by an unrestricted grant from Eli Lilly. We thank personnel from M. D. Anderson Cancer Center (Molecular Therapeutics). The input of Prof. Richard DiMarchi (Indiana University) is gratefully acknowledged.

References

1. Marx V. Chem. Eng. News 2005;83:17–24.
2. Zorko M, Langel U. Adv. Drug Deliv. Rev 2005;57:529–545. [PubMed: 15722162]
3. Richard JP, Melikov K, Vives E, Ramos C, Verbeure B, Gait MJ, Chernomordik LV, Lebleu B. J. Biol. Chem 2003;278:585–590. [PubMed: 12411431]
4. Mason PE, Neilson GW, Dempsey CE, Barnes AC, Cruickshank JM. Proc. Natl. Acad. Sci. USA 2003;100:4557–4561. [PubMed: 12684536]
5. Zahn R, Liu A, Luhrs T, Riek R, von Schroetter C, Lopez Garcia F, Billeter M, Calzolai L, Wider G, Wuthrich K. Proc. Natl. Acad. Sci. USA 2000;97:145–150. [PubMed: 10618385]
6. Huyghues-Despointes BM, Scholtz JM, Baldwin RL. Protein Sci 1993;2:80–85. [PubMed: 8443591]
7. Lee S, Yoshitomi H, Morikawa M, Ando S, Takiguchi H, Inoue T, Sugihara G. Biopolymers 1996;36:391–398. [PubMed: 7669922]
8. Chin D, Woody RW, Rohl CA, Baldwin RL. Proc. Natl. Acad. Sci. USA 2002;99:15416–15421. [PubMed: 12427967]
9. Clarke DT, Doig AJ, Stapley BJ, Jones G. Proc. Natl. Acad. Sci. USA 1999;96:7232–7237. [PubMed: 10377397]
10. Yang JT, Wu CS, Martinez HM. Methods Enzymol 1986;130:208–269. [PubMed: 3773734]
11. Schmidt MC, Rothen-Rutishauser B, Rist B, Beck-Sickinger A, Wunderli-Allenspach H, Rubas W, Sadee W, Merkle HP. Biochemistry 1998;37:16582–16590. [PubMed: 9843425]
12. Fernández A, Berry RS. Proc. Natl. Acad. Sci. USA 2003;100:2391–2396. [PubMed: 12591960]
13. Rief M, Clausen-Schaumann H, Gaub HE. Nature Struc. Biol 1999;6:346–349.
14. Imaba K, Takahashi Y, Ito K, Hayashi S. Proc. Natl. Acad. Sci. USA 2006;103:287–292. [PubMed: 16384917]
15. Oesterhelt F, Rief M, Gaub HE. New J. Phys 1999;1:6.
16. Doi, M.; Edwards, SF. The theory of polymer dynamics. Oxford, UK: Clarendon Press; 1995.
17. Oesterhelt F, Oesterhelt D, Pfeiffer M, Engel A, Gaub HE, Mueller DJ. Science 2000;288:143–146. [PubMed: 10753119]
18. Futaki S, Suzuki T, Ohashi W, Yagami T, Tanaka S. J. Biol. Chem 2001;276:5836–5840. [PubMed: 11084031]
19. Jarzynski C. Phys. Rev. E 1997;56:5018–5024.
20. Jarzynski C. Phys. Rev. Lett 1997;78:2690–2693.

21. Liphardt J, Dumont S, Smith SB, Tinoco I, Bustamante C. Science 2002;296:1832–1835. [PubMed: 12052949]

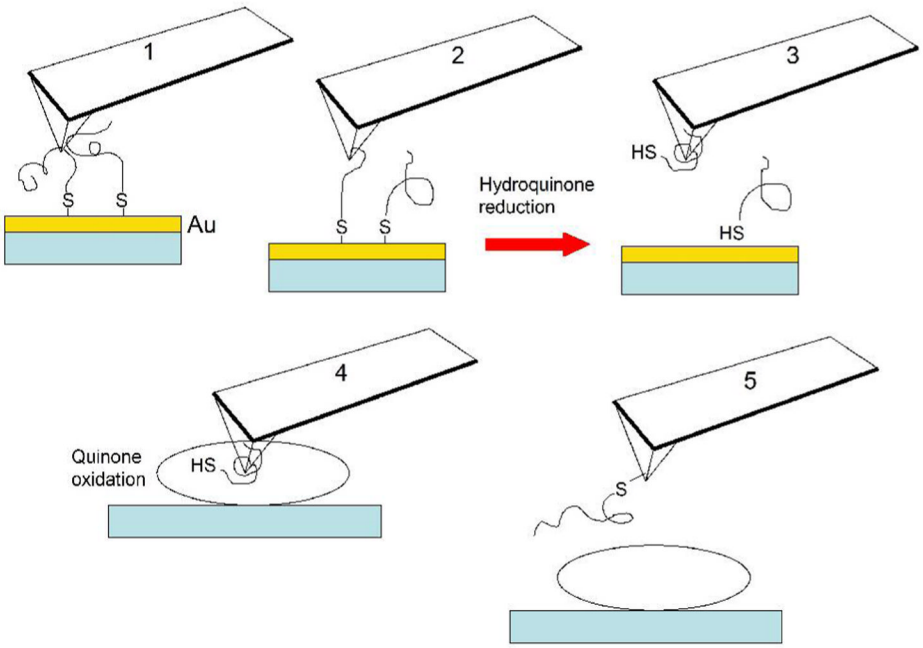

Figure 1.
Scheme of single-molecule tethering to cantilever tip combining five mechanical and redox steps.

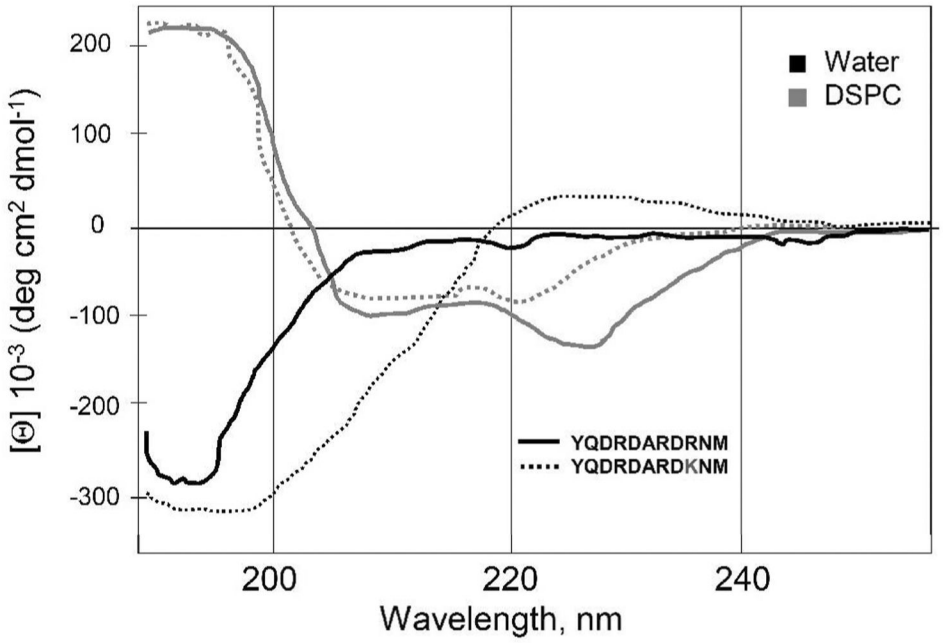

Figure 2.

Environmental effect on the structure of peptides with variable translocation potential determined from far-UV circular dichroism spectra. The mean peptide ellipticity [Θ] for wavelength range 180–280nm was determined in PBS (Dulbecco's phosphate buffer saline solution, pH7.2) and for peptides internalized in DSPC (distearoyl phosphatidylcholine) liposomes. No appreciable ellipticity was detected beyond 260nm. Ellipticity measurements in PBS are plotted in black and those in DSPC, in grey. Peptide **1** is shown in solid lines and peptide **2**, in dotted lines.

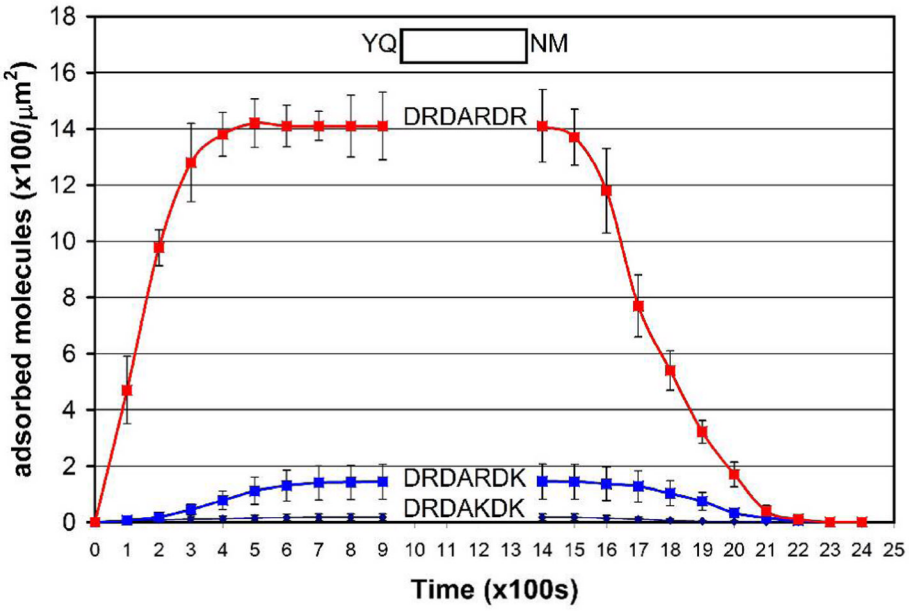

Figure 3.

Adsorption/desorption uptake onto a lipid phase under controlled hydrodynamic conditions determined by evanescent field spectroscopic interrogation of a DSPC Langmuir-Blodgett bilayer. Adsorption took place at constant bulk concentration 1.5 μM (301K, pH7.2), desorption at 0 μM bulk concentration. The kinetics of adsorption/desorption onto and from the bilayer are shown for peptides **1** (red), **2** (blue) and **3** (dark blue). The fixed capping aminoacids are indicated at the top and the peptide sequence yielding polar pairs is given for each curve. Error bars represent dispersions in measured uptake over 5 runs of each assay. On each run, measurements were made every 300s, shifting the first measurement by 100s in each run. A previously designed set-up[12] was adapted to probe lipid insertion for the different peptides. The adsorption/desorption profiles reveal that adsorption equilibration is achieved at t=900s for all peptides. The optimal peptide for delivery across a lipid phase is one with the highest adsorption equilibrium uptake followed by the most complete desorption, as the bulk concentration is reduced from 1.5 to 0 μM within the 900s–1400s interval.

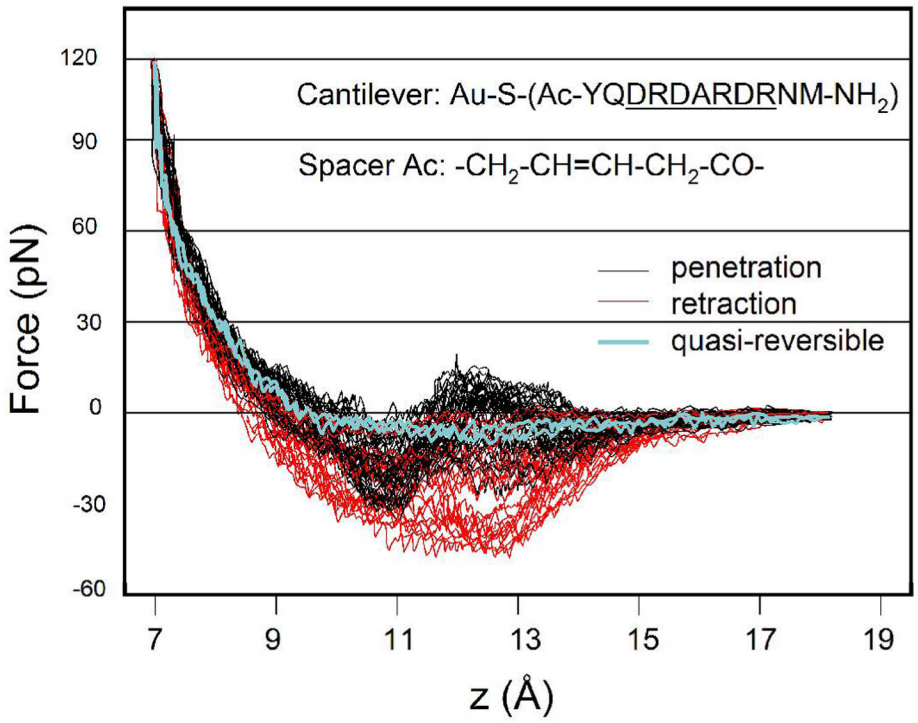

Figure 4.

Deflection force versus cantilever displacement from water-lipid interface (z) for penetration/retraction cycles at steering speed 0.04nm/s with 1s lipid residence time for the functionalized peptide HS-CH_2-CH=CH-CH_2CO-[YQDRDARDRNM]-NH_2 (peptide 1). A single molecule is tethered through a thiolate-gold bond to the gold-coated tip of cantilever BL-RC150VB-HW. The minimal hysteresis cycle (the 29^{th} out of 40 cycles, tip #2 at speed 0.04 nm/s) is displayed by the light blue line.

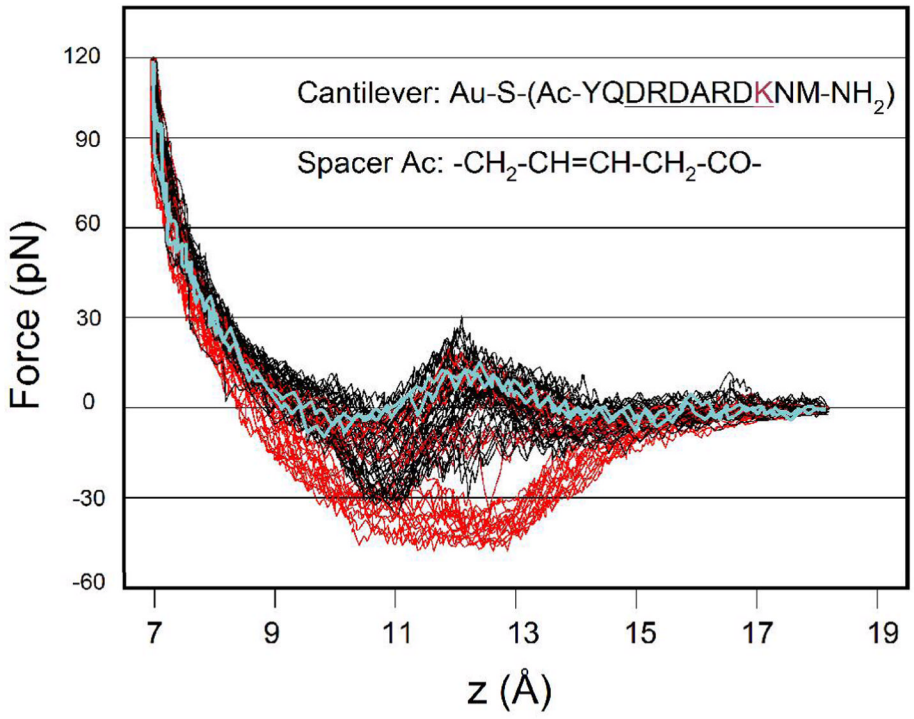

Figure 5.

Deflection force versus cantilever displacement from water-lipid interface (z) for penetration/retraction cycles at steering speed 0.04nm/s with 1s lipid residence time for the functionalized peptide HS-CH_2-CH=CH-CH_2CO-[YQDRDARDKNM]-NH_2 (peptide 2). A single molecule is tethered through a thiolate-gold bond to the gold-coated tip of cantilever BL-RC150VB-HW. The minimal hysteresis cycle (the 33rd out of 40 cycles tip #4 at speed 0.04 nm/s) is displayed by the light blue line.

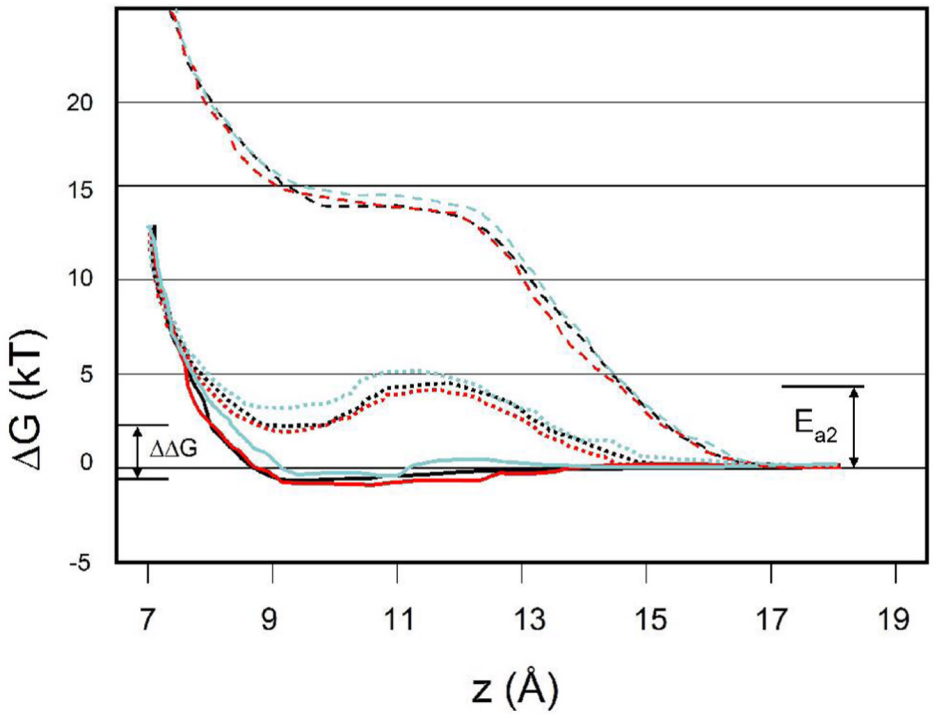

Figure 6.

Free energy profiles for peptide translocation obtained from Jarzynski's equality using the 0.04nm/s manifold of penetration curves (black lines) and retraction curves (red lines) for peptide 1 (solid), 2 (dotted) and 3 (hyphenated). The latter peptide does not insert significantly and thus the cycles show no hysteresis, reflected in the almost coinciding penetration and retraction free energies. An estimation from a minimal-work trajectory extracted from a hysteresis-free cycle is shown in light blue for all three peptides. The thermodynamic and kinetic parameters required for validation against macroscopic measurements are indicated.

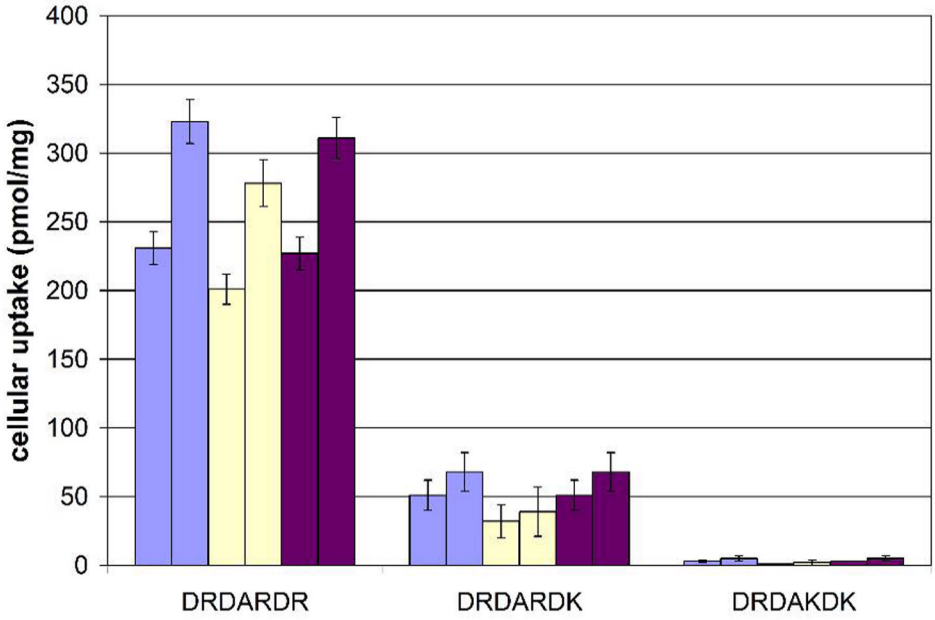

Figure 7.

Peptide internalization measurements revealing the superior translocation efficiency of peptide 1 over translocating peptides 2 and 3. Only the sequence of the salt-bridging region is indicated for clarity. Mouse macrophage RAW264.7 cells were incubated with 1μM fluorescent-labeled peptides for 1h and 4h, then thoroughly washed and lysed. Peptide internalization was assayed by fluorescent measurement on supernatant of centrifuged cell lysate after the 1h and 4h peptide treatment. Error bars represent standard deviations resulting from four independent runs for each measurement. No statistically significant increase in uptake is observed after 4h incubation with the peptides. In controls, the isolated rhodamine fluorophore and labeled random peptides were assayed, revealing no translocation or membrane penetration. Blue bars indicate peptide uptake on cells incubated as described in Methods, yellow bars indicate uptake on cells treated with trypsin, and magenta bars represents uptake on cells incubated with sodium azide (Methods). The left-hand bar of each type corresponds to 1h incubations with the labeled peptide, while the right-hand bar corresponds to 4h-incubations under the same conditions. Trypsin digestion enables an estimation of the extent of peptide internalization excluding membrane-bound peptides. The sodium azide treatment depletes cellular ATP, and a high impact on uptake would suggest endocytosis as a dominant mechanism for internalization.